Quantifying the Shapes of U.S. Landfalling Tropical Cyclone Rain Shields*

Corene Matyas
University of Florida

Tropical cyclones (TCs) produce complex rainfall patterns that are difficult to predict due to atmospheric and land surface forcings. This study utilizes geographic information systems to spatially analyze radar returns and calculate several metrics that quantify the shapes of TC rain shields. Three stepwise discriminant analyses are performed to determine which of the shape metrics distinguish among TCs categorized by: intensity, distance traveled inland, and orientation of terrain encountered. Results confirm that TC rain shields often assume noncircular shapes. Utilizing shape indices to model rain shields could help produce TC rainfall forecasts that are more spatially accurate. **Key Words: GIS, radar, rainfall, shape analysis, tropical cyclones.**

Tropical cyclones (TCs) are dangerous storms capable of producing strong winds, storm surges, tornadoes, and flooding rainfall. Prior to 1970, the storm surge caused the majority of TC-related deaths (Rappaport 2000). Fortunately, improvements in track and intensity forecast models (Aberson 1998) now allow time for the evacuation of surge-prone areas, which has reduced the number of surge-related deaths. More recently Rappaport found that during 1970–1999, heavy rainfall and its associated flooding accounted for 59 percent of deaths caused by TCs. The fact that TCs can produce excessive rainfall many kilometers inland from the coast increases the portion of the population that is vulnerable to this hazard. For example, flooding caused by Tropical Depression Charley (1998) resulted in twenty deaths near Del Rio, Texas, located more than 350 km from the point of landfall (Pasch, Avila, and Guiney 2001). As recently as 2000, the American Meteorological Society acknowledged that "skillful prediction of rainfall from landfalling tropical cyclones remains elusive" (AMS 2000, 1344). To reduce the loss of life and property damage caused by this freshwater flooding, models must be developed that accurately forecast the amount and spatial extent of rainfall produced by landfalling TCs.

The development of a rainfall climatology and persistence model (R-CLIPER; Marks, Kappler, and DeMaria 2002) facilitated the validation of rainfall forecasts for TCs (Marchok, Rogers, and Tuleya 2007). To develop this model, researchers divided each TC into sections using fifty 10-km wide annular rings and then calculated the average rainfall rate within each ring. The rainfall distribution generated by the R-CLIPER model is symmetrically-shaped with maximum rain rates approximately 50 km from the storm center. Due to a distance-decay assumption, the R-CLIPER model predicts a steady decrease in rainfall rates as the TC tracks inland. However, researchers have noted that many TCs produce rainfall that is heavily concentrated to one side of the storm track (Gilbert and LaSeur 1957; Elsberry 2002; Corbosiero and Molinari 2003). Also, topographical features or the interaction with middle latitude weather systems can act to both increase rainfall and cause the shape of the rain shield to become asymmetrical (Bender, Tuleya, and Kurihara 1985; Lin et al. 2002; Atallah and Bosart 2003). A successful TC rainfall forecast must incorporate these asymmetrical shapes.

Improving the spatial accuracy of TC rainfall forecasts requires the ability to model how the

*Partial funding for this research was provided by a fellowship from the Society of Women Geographers. Assistance in securing the radar data by Rebecca Yothers and the Pennsylvania State University Department of Meteorology was greatly appreciated, as was the georeferencing script provided by Scott Shipley, and the support given by Andy Sherwood. Thanks are also extended to Tim Fik for his assistance in revising an early draft of this article, and to four anonymous reviewers. Finally, I thank my advisor, Andrew Carleton, and committee members Brent Yarnal, Jenni Evans, and Donna Peuquet for their time and insights into this work.

The Professional Geographer, 59(2) 2007, pages 158–172 © Copyright 2007 by Association of American Geographers.
Initial submission, April 2006; revised submission, August 2006; final acceptance, October 2006.
Published by Blackwell Publishing, 350 Main Street, Malden, MA 02148, and 9600 Garsington Road, Oxford OX4 2DQ, U.K.

atmosphere and land surface influence the shape of the rain shield. A TC that tracks inland, rather than moving parallel to the coastline or moving back over the ocean, becomes removed from its source of moisture. The reduction in moisture alters the storm structure (Tuleya 1994) and leads to a decrease in rainfall. If moist air continues to enter the TC, as described by Bluestein and Hazen (1989) for Hurricane Alicia (1983), rainfall may occur on one side of the storm only, yielding an elongated rain shield shape. Also, TCs making landfall in the United States tend to have a northward component to their motion, which allows approaching middle latitude features to alter rain shields into noncircular shapes (Atallah and Bosart 2003).

The task of quantifying changes in shapes lends itself to geographers, who explore various types of spatial data with tools such as geographic information systems (GIS) and shape analysis (MacEachren 1985; Wentz 2000). The research objectives of this article are twofold: (1) utilize GIS and shape analysis to quantify changes in the shapes of the rain shields of landfalling TCs; and (2) determine the specific shape indices that quantify alterations of the rain shield caused by land surface and atmospheric forcing mechanisms. This article investigates three such mechanisms: storm intensity, the distance inland over which the storm moves, and the orientation of elevated topography encountered by the storm. If the shape indices calculated in this study can successfully model the way in which a TC's rain shield changes, their inclusion in a rainfall forecast model could improve predictions of where flood-producing rainfall is likely to occur.

As spatial analysis requires high-resolution data, the following section discusses how base reflectivity radar returns are utilized in this study. The primary objective of this research is to define the shapes of the rain shields as indicated by the radar data. Two techniques that facilitate this task: (a) overlaying each hourly radar composite with a circular grid; and (b) performing shape analysis are then described in the next section, Spatial Analysis. When developing the R-CLIPER model, Marks, Kappler, and DeMaria (2002) employed a circular grid to section each TC. In the current study, a circular grid divides each TC into sections, and the percentage of area within each section that is covered by radar returns is calculated. For the second technique, three measures of shape frequently employed by geographers (Stoddart 1965; Frolov 1975; DeMers 2000) are calculated to quantify changes in the shape of the rain shield: the area-to-perimeter ratio (APR), the major-to-minor axis ratio (MMR), and the Euler number (EN). These indices are calculated to determine the compactness, elongation, and fragmentation of the rain shield. An additional shape metric, the rain shield arc-length, quantifies the degree to which the rain shield encircles the storm center.

The Statistical Analysis section describes how discriminant analyses (DAs) are employed to accomplish the second objective of this research, which is to identify the grid sections or shape indices, or both, that best quantify how the spatial extent of TC rain shields are affected by the atmosphere and the land surface. Three separate DAs are performed to determine which of the grid sections and/or shape indices best differentiate between (1) TCs of hurricane (tropical storm) intensity; (2) TCs whose circulation centers are inland and located near to (far from) the coastline; and (3) TCs encountering elevated topography that is oriented in different directions. The final two sections of this article discuss the results of the DAs and address the potential for the shape indices calculated in this study to be incorporated into a TC rainfall forecast model.

Data and Methods

The Weather Surveillance Radar 88 Doppler (WSR-88D) level II radar data utilized in this research were obtained from the Pennsylvania State University Department of Meteorology (PSUDM). These base reflectivity radar returns are obtained in bins of varying resolution out to 235 km from the receiver for each degree of the 360° scan (Klazura and Imy 1993). The radar data are georeferenced utilizing Nex2SHP.exe, a Visual Basic script (Shipley, Graffman, and Ingram 2000), and imported into ArcView GIS (ESRI 2002). Twelve TCs from 1997–2003 are analyzed (these are listed in Table 1 in order of maximum sustained winds). Changes in the formatting of radar data (Kruger and Krajewski 1997) do not allow the Nex2SHP.exe script to decode data prior to 1997. Alterations to the compression algorithms used by PSUDM to store radar data do not allow Nex2SHP.exe to recognize data from years 2001 and 2002. The

Table 1 *Characteristics of analyzed tropical cyclones at time of landfall*

Tropical cyclone (year)	Minimum central pressure (mb)	Maximum sustained winds (m/s)	Forward motion (degrees/m/s)	Average gale-force wind radius (km)
Bret (1999)	951	51.4	285/3.2	194
Bonnie (1998)	964	48.9	20/2.7	196
Isabel (2003)	957	46.3	325/8.8	405
Georges (1998)	964	46.3	345/3.2	225
Claudette (2003)	979	41.2	285/6.5	194
Danny (1997)	984	36.0	25/1.1	–
Irene (1999)	987	36.0	30/6.1	220
Dennis (1999)	984	30.9	305/4.3	185
Gordon (2000)	991	28.3	20/6.9	135
Charley (1998)	1000	20.6	295/4.6	194
Hermine (1998)	1000	18.0	360/1.0	58
Helene (2000)	1006	18.0	45/5.8	91

author obtained data from NOAAPORT data broadcast system for Claudette (2003) and Isabel (2003) as these TCs made landfall, thus bypassing the data compression process. Data files from TCs Earl (1998), Frances (1998), and Floyd (1999) were corrupted and could not be analyzed.

Radar returns from the scan nearest the top of each hour for each station are composited into one layer containing data from all stations. The interpolation of these data by inverse distance weighting creates the polygons that define the spatial boundaries of the rain shield. To obtain a completely closed polygon, the entire rain shield must be within receiving range of the radar station(s). This criterion determines when analysis commences or ceases for each TC. Partial polygons are not analyzed. A total of 486 hourly observations are analyzed in this manner from twelve U.S. landfalling TCs (Figure 1).

Selection of the reflectivity threshold from which these polygons are created is important as it affects the resulting shapes. TC researchers have employed both 20 dBZ (Jorgensen 1984; Toracinta et al. 2002) and 25 dBZ (Barnes et al. 1983; Powell 1990) reflectivity values to define the boundaries of TC rain shields and individual rain bands. Reflectivity values less than 20 dBZ may result from insect swarms or flocks of birds (Klazura and Imy 1993) and are not suitable for the current study. Polygons created from both the 20 dBZ and 25 dBZ contours were compared by Matyas (2005). These analyses revealed that shape measures calculated from the 20 dBZ contours produced statistically significant results that superseded those produced by the 25 dBZ polygons, as the latter were highly fragmented and small in size. For brevity, this article only discusses shape metrics calculated from the polygons bound by 20 dBZ contours.

The National Hurricane Center (NHC) provides additional data for each TC, including the coordinates of the circulation center, maximum sustained wind speed, and minimum central pressure. These observations are available in six-hourly increments. As this study analyzes the radar images in hourly increments, it is necessary to interpolate the NHC-provided data (Vickery, Skerlj, and Twisdale 2000). Within this article, observation times are referenced to the hour of landfall (e.g., $t+0$ for the landfall hour, $t+6$ for six hours postlandfall, etc.) Also, as three TCs made multiple U.S. landfalls, the following locations serve as the referenced landfall points: Fort Morgan, Alabama, for Hurricane Danny (1997); Biloxi, Mississippi, for Hurricane Georges (1998); and Cape Sable, Florida, for Hurricane Irene (1999).

Spatial Analysis

To ascertain whether the technique used to develop the R-CLIPER model provides adequate information from which to model the shape of a TC rain shield, a set of annular rings divided into quadrants is placed over each rain shield (Matyas 2006). Within the GIS, the circulation center of the storm is buffered by eight rings spaced 50 km apart. The heading of the storm determines where each quadrant is located. This circular grid (Figure 2) clips the original polygons into new shapes, whose areas are summed to determine the amount of space

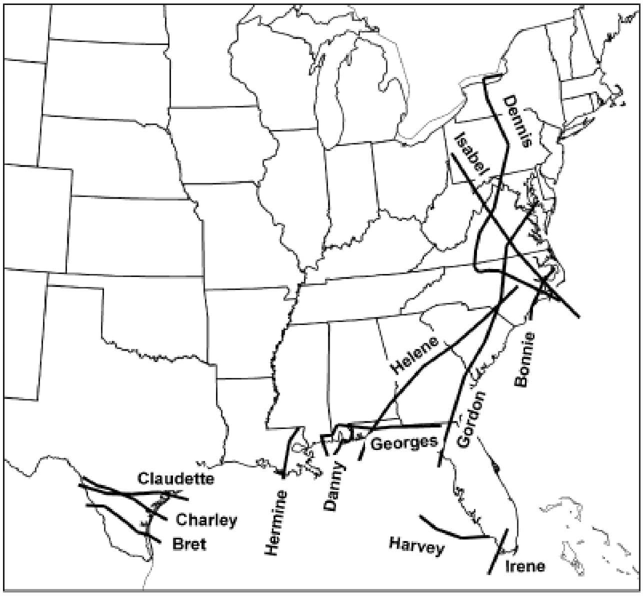

Figure 1 *Hourly locations of storm circulation center for each tropical cyclone in this study.*

within each region that is covered by the 20 dBZ reflectivity threshold. As each annular ring encloses a different amount of space, the percentage of space occupied by polygons between each pair of rings is calculated. Hereafter, the region inside of ring 1 is referred to as R1, the region between rings one and two is R2, and so forth (Figure 2). Summing the areas of all polygons in the image determines the total areal extent of the rain shield. The total area of the polygons

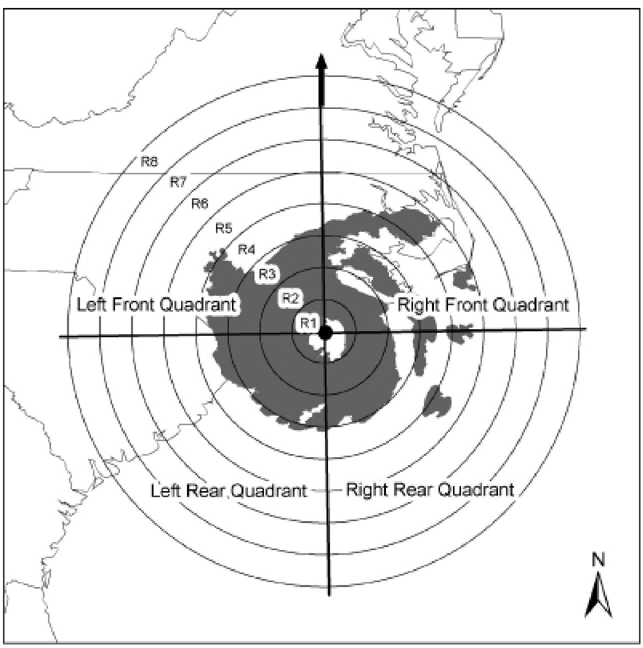

Figure 2 *Buffered 50 km annular rings and quadrants used to clip the rain shield polygons. Storm motion is toward the north-northeast.*

inside each quadrant is also calculated. Additionally, as researchers have noted the tendency for TCs to produce precipitation that is asymmetrical to the storm track (Elsberry 2002; Chan and Liang 2003), the areas of all polygons on the left side of the storm track are summed and subtracted from those on the right side of the track. When the value of this right-minus-left asymmetry (RLSYM) variable is negative (positive), more of the rain shield exists on the left (right) side of the storm.

Previous researchers have determined the spatial distribution of precipitation about a TC's center using grids of varying dimensions (Rao and Macarthur 1994; Rodgers, Chang, and Pierce 1994; Cerveny and Newman 2000). However, the development of a model that predicts changes in TC shape properties should also quantify the rain shield as a whole. To accomplish this task, three geographical measures of shape are examined (Matyas 2007): area-to-perimeter ratio (APR), major-to-minor axis ratio (MMR), and Euler number (EN). The APR, which is calculated for the largest polygon in each image, provides a simple measure of storm compactness:

$$APR = \sqrt{A}/(P \cdot 0.282), \tag{1}$$

where A is the area inside each polygon, and P is the perimeter of each polygon (Figure 3). The MMR describes whether the rain shield is circular or elongated (Figure 4). This measure is calculated relative to the geographical centroid of all polygons comprising the rain shield. Radial lines are extended out from the centroid to the edges of the polygons. The longest line, determined by summing the length of each line with that extending 180° away from it, serves as the major axis of the rain shield (L_{maj}). The radials located 90° to each side are summed to calculate the minor axis length (L_{min}). The minor axis length is divided by the major axis length to produce the MMR.

$$MMR = L_{min}/L_{maj}. \tag{2}$$

Both the APR and MMR values range from zero to one and compare the rain shield's shape to that of a circle, which has an APR and MMR value of one. The EN accounts for both the number of polygons present (fragmentation)

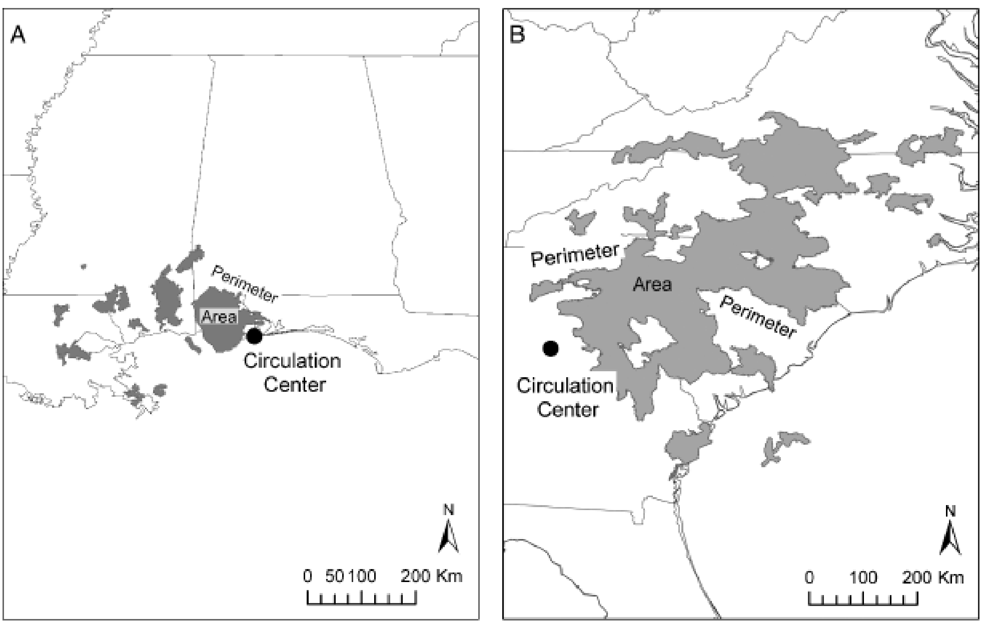

Figure 3 *Examples of the area-to-perimeter ratio (APR) compactness measure. (A) is a compact rain shield shape from Danny (1997) where area is maximized (APR = 0.54). (B) is a linear shape from Helene (2000) where perimeter is maximized (APR = 0.14).*

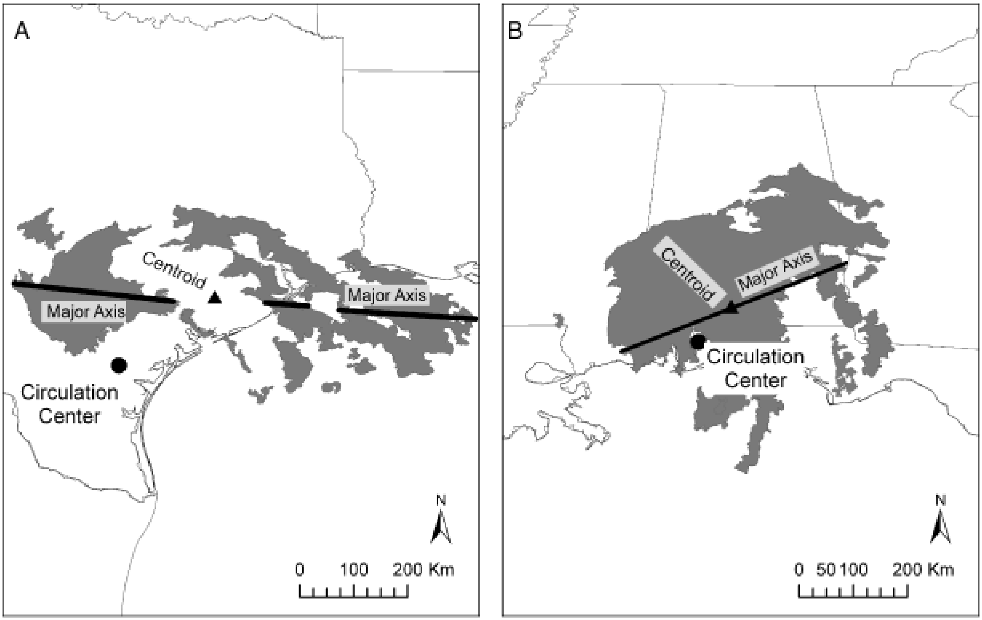

Figure 4 *Examples of (A) elongated (MMR = 0.19; Charley 1998) and (B) round (MMR = 0.89; Georges 1998) rain shield shapes. MMR = major-to-minor axis ratio.*

and holes within the polygons (perforation):

$$EN = H - (F - 1), \quad (3)$$

where H is the number of holes and F is the number of fragments in the examined region (Figure 5). A negative EN value indicates a fragmented shape.

One additional measure of shape that considers the entire TC rain shield is developed specifically for this study. This shape metric quantifies the degree to which the rain shield encircles the circulation center of the storm, and is hereafter referred to as the rain shield arclength (RSAL). TCs containing plentiful moisture and fast winds can advect moisture around the entire 360° arc. Reflectivity values greater than 20 dBZ may only exist around half of the arc (180°) if TCs have slower winds, are advecting dry air into their circulation (Gilbert and LaSeur 1957), or experience strong directional wind shear (Corbosiero and Molinari 2002). To calculate the RSAL metric, radial lines are extended outward in 5° increments from the coordinates of the TC circulation center. The degrees of the radial lines that encounter the leading and trailing edges of the rain shield are subtracted to provide the RSAL (Figure 6).

Statistical Analysis

Three forward stepwise linear discriminant analyses (DAs) are performed to determine which of the predictor variables (Table 2) best relate changes in TC rain shields due to storm intensity (DA1), distance inland (DA2), and the orientation of elevated terrain (DA3). DA is similar to linear regression analysis; the main difference is that DA predicts membership in two or more mutually exclusive groups from a set of predictor variables (Saunders et al. 2000). The twenty-two predictor variables (Table 2) consist of the areal coverage of rain derived from the circular grids and the geographical shape indices for all TCs in six-hourly increments beginning with the hour of landfall. The inclusion of hourly observations in the statistical analysis is problematic due to temporal autocorrelation. The use of six-hourly data is justified in this study because a TC's circulation changes rapidly once landfall commences as compared to that while over open water. Therefore, the use of six-hourly observations reduces temporal autocorrelation in the data.

Through a linear combination of the predictor variables, the DA derives a function that

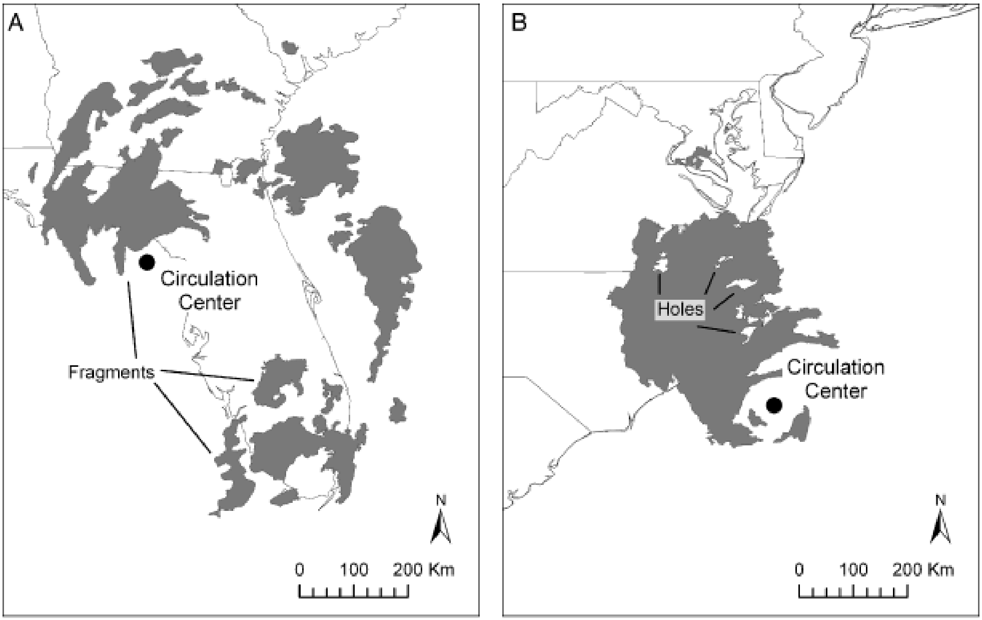

Figure 5 *Examples of Euler number calculations for (A) Gordon (2000; EN = −15) and (B) Dennis (1999; EN = 2).*

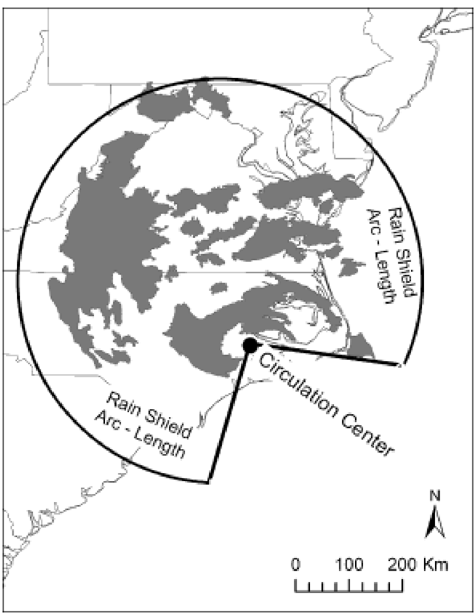

Figure 6 *Calculation of the rain shield arc-length (285°) for Dennis (1999) at six hours post-landfall.*

maximizes the separation of the groups. Given that many environmental forcing mechanisms can simultaneously affect a TC's rainfall production (e.g., interaction with middle latitude weather systems while moving over mountainous terrain), it is appropriate to place the observations in this study into groups rather than attempt to predict the precise value of the dependent variable. The large number of predictors in these analyses (Table 2) dictates the use of stepwise DA. The predictor that is included in the model at each step is the one that decreases the Wilks's Lambda statistic by the greatest amount (Tabachnick and Fidell 2001). This statistic varies between zero and one and is a measure of the difference between groups of the centroid of means on the independent variables. Values near zero indicate that the group means differ. Each step in the analysis adds a variable to the model that most increases the distance between the group centroids.

Two techniques validate the classification accuracy of the model produced by each DA. First, the performance of a jackknife data-resampling procedure ensures that the analysis results are not biased toward any one TC (DeMaria and Kaplan 1994). This procedure removes one sample at a time and recalculates the model

Table 2 *Predictor variables entered into all discriminant analyses*

Variable type	Listing			
Circular grid	Area of rain shield in RR, RF, LF, LR quadrants	Percentage of region occupied by rain shield in R1, R2, etc.	Total areal extent of rain shield	Right minus left asymmetry (RLSYM)
Shape indices	Major-to-minor axis ratio, area-to-perimeter ratio; Euler number	Distance and bearing of shield centroid from storm center	Orientation of major axis (ORI)	Rain shield arc-length (RSAL)

Note: RR = right rear, RF = right front, LF = left front, LR = left rear; R1 = radius 1, R2 = radius 2.

statistics until all samples have been cross-validated. Second, a random selection of observations from each group is entered into the analysis without prior group classification. The DA then constructs a model from the observations that are classified and uses that model to predict group membership for all observations that had not been classified originally. A high percentage of observations that are correctly classified using both the jackknife procedure and the data that are manually withheld indicate model success.

The intensity of a TC has important influences on its cloud formation, leading Dvorak (1975) to forecast storm intensity by classifying the shapes of clouds observed on satellite imagery. It is reasonable to assume that intensity will also affect the shape of the rain shield as viewed on radar imagery. Faster tangential winds can carry moisture completely around the inner core of a hurricane, whereas slower winds in tropical storms may not allow moisture to encircle the storm's center. Therefore, faster winds should be associated with a more circular rain shield shape. This study stratifies TCs into two groups for DA1 (Table 3): those having winds above and below hurricane-force (33 m/s). To eliminate problems associated with "borderline" observations, cases with wind speeds of 31–35 m/s are not included in the analysis. Observations included in the two groups are from the hour of landfall and six hours after landfall. After $t + 6$, most storms contained weak tropical storm or tropical depression-force winds. The results of additional DAs incorporating data through $t + 24$ (not shown) indicate that intensity is not a dominant control of the rainfall distribution after $t + 6$.

As a TC migrates inland, the circulation center is removed from the warm ocean waters that provide the energy required to maintain the circulation (Hubert 1955; Tuleya and Kurihara 1978; R. W. Jones 1987); as a result the shape and the extent of the rain shield change. Some TCs, however, remain near the coastline after landfall, or migrate across the coastline after spending several hours over land. Being located near warm ocean waters allows for the continual advection of moisture into a TC's circulation, and this may allow for coastal TCs to be more symmetrical in shape or to have a larger rain shield than inland TCs. For DA2, observations from $t + 6$ to $t + 36$ are placed into two groups: those within 100 km of the coastline, and those located more than 200 km from the coastline (Table 3). This distance is determined by measuring the distance between the circulation center of the TC and the nearest point on the coastline, not the coordinates of landfall. The 100- and 200-km distances are chosen to delineate the categories because they represent natural breaks in the data.

Researchers have documented how orographic uplift can enhance precipitation on the right side of a TC relative to storm motion (Bender, Tuleya, and Kurihara 1985; Wood 2001; Lin et al. 2002). As a TC approaches elevated terrain at a perpendicular angle, its rain

Table 3 *Group membership for each discriminant analysis (DA)*

Group	Grouping criteria		
	Intensity DA1	**Distance inland DA2**	**Topography DA3**
1	Wind speed > 35 m/s (12 cases)	< 100 km of coastline (23 cases)	Edwards Plateau in Texas (east-west orientation) (14 cases)
2	Wind speed < 31 m/s (10 cases)	> 200 km from coastline (17 cases)	Appalachian Mountains (northeast-southwest orientation) (15 cases)

Table 4 *Results of each discriminant analysis (DA)*

	Intensity (DA1)	Distance inland (DA2)	Topography (DA3)	
Predictor(s)	RSAL	MMR	ORI RLSYM	
Group 1.				
Mean	349°	0.67	278°	57
SD	39°	0.10	26°	34
	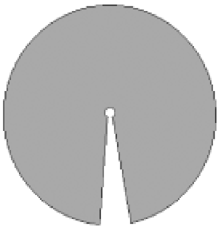	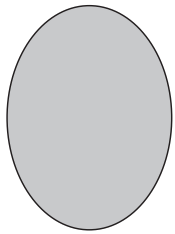	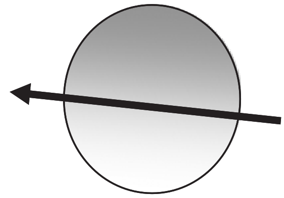	
Group 2.				
Mean	171°	0.31	41°	–25
SD	45°	0.09	20°	58
	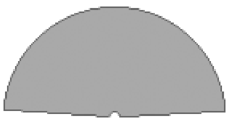	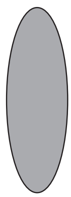	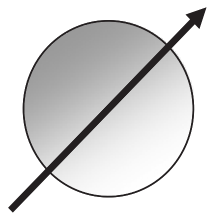	
Wilks's Lambda (significance)	0.169 (0.000)	0.267 (0.000)	0.193 (0.000)	
Percentage of correct cases	95.5%	95%	100%	

Note: RSAL = rain shield arc-length; MMR = major-to-minor axis ratio; ORI = orientation of major axis; RLSYM = right minus left asymmetry; SD = standard deviation.

shield should become asymmetrical, with increased (decreased) areal coverage on the right (left) side of the storm. The shield's major axis should also become oriented in a direction parallel to the axis of the elevated terrain. In this study, several TCs encountered elevated terrain in two regions of the United States: the Appalachian Mountains (northeast-southwest orientation) in North Carolina, Virginia, West Virginia, Maryland, Pennsylvania, and New York, and the Edwards Plateau (east-west orientation) in central Texas (Figure 7). For DA3, observations taken from $t+12$ to $t+24$ for seven TCs are grouped according to these two regions (Table 3).

Results and Discussion

The models developed by all three DAs utilize one or two predictors to correctly classify 95 percent or more of the cross-validated and manually-withheld observations. The predictors for all three models consist of shape indices that consider the rain shield as a whole, rather than the variables derived from the circular grid. The graphics developed to illustrate the representative shapes of each group according to the model predictors of all three DAs (Table 4) illustrate that a circle is not a representative shape for all TC rain shields. These findings demonstrate that future TC rainfall forecast models need to consider non-circular rain shield shapes and indicate that shape metrics can be utilized to model these asymmetrical rain shield shapes. Having such a high success rate also validates the technique of using a GIS to spatially analyze radar reflectivity returns. The details of each DA are discussed below.

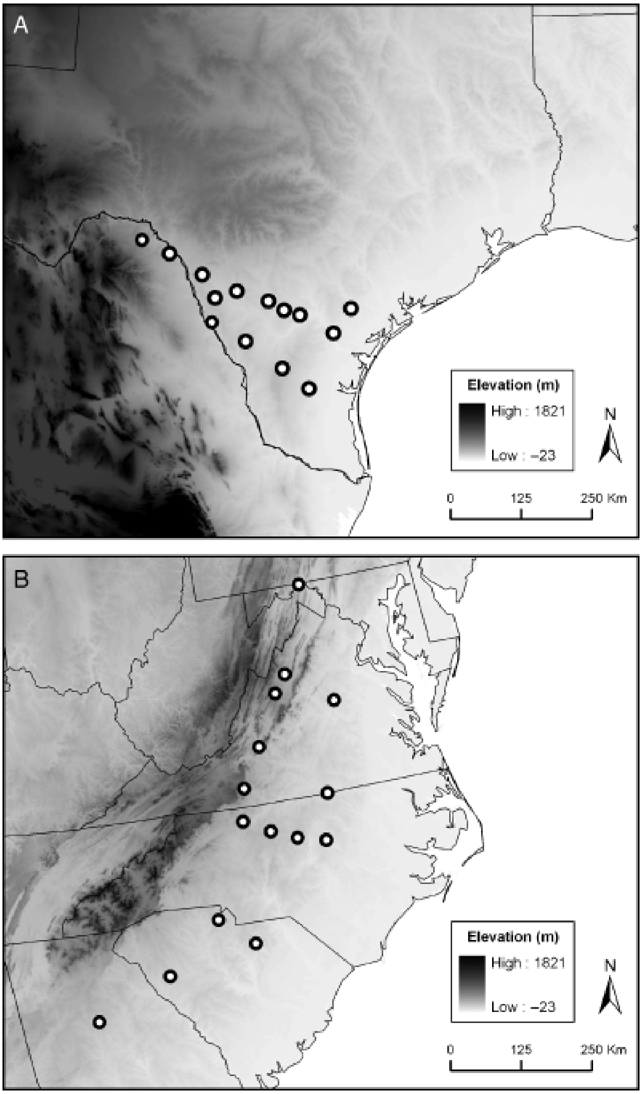

Figure 7 *Elevation map depicting the observations utilized in DA3 for (A) the Edwards Plateau in central Texas and (B) the Appalachian Mountains. Circles denote storm center positions. DA = discriminant analysis.*

Intensity and an Enclosed Circulation Center

The intensity DA model only requires one predictor, the RSAL, to distinguish between hurricane and tropical storm rain shields. The mean values of RSAL for each group indicate that hurricane rain shields nearly enclose their circulation centers (Table 4). This is in stark contrast to tropical storm rain shields, where the average RSAL is only 171°. The lower RSAL value for tropical storms is likely due not only to slower tangential winds caused by a weakening pressure gradient force, but also to the strong directional wind shear that the storms in this study experienced during landfall (Franklin et al. 2001; Lawrence et al. 2001; Pasch, Avila, and Guiney 2001). When directional wind shear acts on TCs, vertical circulation becomes asymmetric as upward (sinking) motions are induced downshear (upshear) (Black et al. 2002). Sinking motion inhibits convection. The weakening of tangential winds also prohibits moisture from completely circulating around the storm. As a result, precipitation is displaced downshear left of the circulation center (Rogers et al. 2003). As many TCs experience strong directional wind shear prior to and/or after landfall, it is important to model the changes in TC rainfall patterns caused by this forcing mechanism and to determine to what extent the RSAL is capable of quantifying these changes. Future work will focus on the development of a shape metric specific to wind shear–generated rain shield asymmetries.

Only one observation is misclassified by DA1. Hurricane Isabel began to transition into an extratropical storm (Gautam et al. 2005) at $t+6$, which caused its rain shield to assume an asymmetrical shape. During this transition, the storm changed from a symmetrical warm-cored to an asymmetrical cold-cored system (Hart and Evans 2001). An area of increased rainfall occurred near the steep thermal gradient between the tropical and continental air masses typically located north of the storm's center (Klein, Harr, and Elsberry 2000; S. C. Jones et al. 2003). For Isabel, this process caused 94 percent of its rain shield to be displaced ahead of the circulation center even though its maximum sustained wind speed was still 36 m/s. As a result, its RSAL decreased to 225° from 360° six hours earlier. Although tropical storms Dennis (1999) and Gordon (2000) also experienced an extratropical transition, this study currently does not possess enough observations from TCs that experienced this transition to investigate the related rain shield shape changes through statistical analysis. However, this transition is a critical factor that needs to be incorporated into future TC rainfall forecast models, and combinations of shape indices such as RLSYM and RSAL may be able to model these storms.

Distance from the Coastline and Elongated Tropical Cyclones

Results from DA2 indicate that TCs located within 100 km of the coastline have a more circular shape than those located more than 200 km inland, which are more elongated. Ninety-five percent of the observations are correctly classified using one predictor (MMR). An examination of the mean MMR for each group reveals that TCs located closer to the coastline are twice as circular, on average, as those further inland (Table 4). This result has important implications for the development of a rainfall forecast model because it illustrates that it is important to model the shape of the entire rain shield as a whole by utilizing shape measures such as the MMR, as analyzing individual segments of the shield would not have produced this result.

The DA2 models developed with the jackknife technique and the randomly-withheld observations misclassify one case from each group. Claudette was 365 km inland at $t+18$, yet it is classified as a coastal storm because its MMR value (52) was the highest of the inland group. The $t+6$ observation for Charley is mistakenly categorized as inland by DA2 when it is located 83 km from the coastline because it has an MMR value of 37. Charley retains a very elongated shape throughout landfall (Figure 4) because the strong directional wind shear it experiences does not allow moisture to completely encircle the circulation center of a TC. During the thirty-eight hours after landfall in which shape indices are calculated for Charley, the polygons located on the right side of the storm track comprise 88 percent or more of the entire rain shield, illustrating that an elongated shape is not necessarily centered over the storm track, as the R-CLIPER model currently predicts. Both of these facts demonstrate the complexity that a successful TC rainfall forecast model must possess as it must account for multiple forcing mechanisms, such as an inland location, strong directional wind shear, and movement over elevated terrain (DA3) that can occur simultaneously.

Topography's Effect on Tropical Cyclone Orientation

TCs encountering the east-to-west (northeast-to-southwest) oriented Edwards Plateau in central Texas (Appalachian Mountains) have rain shields that are also oriented east-to-west (northeast-to-southwest), as confirmed by DA3 (Table 4). Adding a second predictor, RLSYM, reduces the Wilks's Lambda statistic to 0.193, the lowest attained in this study (Table 4). It is not surprising, therefore, that all observations withheld using the jackknife technique and observations that were randomly withheld are correctly classified by the DA3 model. Again, this finding demonstrates that it is necessary to use shape measures that consider the characteristics of the entire rain shield when relating changes in the rain shield to atmospheric and land surface forcing mechanisms. It also illustrates that a model must incorporate measures of asymmetry, rather than assume a circular shape, to more accurately forecast the rainfall patterns of landfalling TCs.

At first glance, the fact that the TCs tracking near the Appalachian Mountains have more of their rain shield on the left side of their circulation center seems to contradict previous research, which indicates that a TC encountering mountainous terrain experiences increased precipitation on its right side due to orographic uplift (Bender, Tuleya, and Kurihara 1985). However, this scenario only holds true if the storm moves in a direction perpendicular to the axis of the elevated terrain. Gordon and Helene tracked parallel to the Appalachian Mountains (Figure 1), causing moisture advected from the Atlantic Ocean to be uplifted by the topography on the left side of the storm track. Additionally, other forcing mechanisms may influence the storm. TCs that migrate into higher latitudes are influenced by middle latitude weather systems. As previously mentioned, Dennis, Gordon, and Isabel become extratropical cyclones while over the United States. During this transition, the maximum precipitation amounts shift to the left front quadrant of the storm (Ritchie and Elsberry 2001; Atallah and Bosart 2003), causing predictor RLSYM to have a negative value. Again, this finding illustrates that multiple precipitation-altering processes affect TCs and that these interactions between the atmosphere/land surface and TCs warrant further investigation before an accurate rainfall forecast model can be developed.

Conclusions and Future Research

This study employs a GIS to examine how storm intensity, distance inland, and topography can affect the shapes of TC rain shields. Changes in these shapes are quantified by dividing the storm into segments, a method employed by previous TC researchers, and by calculating several indices of shape that consider the rain shield as a whole, a method employed by geographers. Three separate DAs then determine which of these variables can best distinguish between TCs of hurricane or tropical storm intensity, TCs located within 100 of or over 200 km from the coastline, and TCs tracking near the Appalachian Mountains or encountering elevated terrain in Texas. As shape indices, rather than regions of the storm defined by the annular rings, were the key predictors in the DAs, this study demonstrates that it is important to consider how the shape of the entire rain shield is changing, rather than just analyzing individual segments. This study also shows that the geographical measures of shape calculated in this study are capable of quantifying these changes in shape.

The three DA models described in this article produce statistically significant results by utilizing shape metrics that quantify aspects of the entire rain shield to predict group membership. The specific relationships between the atmosphere/land surface and the changes in shape are as follows:

- As hurricanes have faster winds that advect moisture completely around their circulation centers, they have a high RSAL (349°). Tropical storms have slower winds and may be affected by strong directional wind shear that limits the arc-length of their rain shield to an average of 171°.
- TCs remaining within 100 km of the coastline exhibit a more circular shape (average MMR 0.67) than do those located more than 200 km inland (average MMR 0.31) as quantified by the MMR.
- When TCs encounter elevated terrain, the orientation of their rain shields parallels that of the axis of the elevated terrain (average ORI of 278° for the east-west Edwards Plateau, average of 41° for the northeast-southwest Appalachian Mountains). TCs tracking near the Appalachian Mountains are also influenced by middle latitude weather systems that shift the rain shield to the left side of the storm track (negative RLSYM).

These findings also demonstrate that TC rain shields often assume asymmetrical shapes. The shape measures calculated in this study are capable of quantifying these shapes and could be employed to improve future TC rainfall forecasts.

To strengthen the findings of this study, future research will investigate changes in the rain shield shapes of additional TCs. Recent technological developments (Ansari and Del Greco 2005) will allow the examination of storms beginning with the 1995 season up to present day, for a total of more than fifty U.S. landfalling TCs. This increased sample size will allow TCs to be stratified according to the various forcing mechanisms that affect them, including several forcing mechanisms mentioned but not examined in this study (e.g., extratropical transition, wind shear). The shape measures described in this article, along with other metrics not discussed here, will be calculated and used to model changes in the rain shield. The ultimate goal of this research is to develop a TC rainfall model capable of combining data from a climatology of rain shield shape changes specific to each physical forcing mechanism with data pertaining to a current storm's history collected via pre-landfall satellite imagery to predict the shape of its rain shield at landfall and throughout the post-landfall period. The forecasted shape could then be input into hydrological models that already operate within a GIS (Vieux 2001) to improve predictions of where freshwater flooding will occur. The evacuation of flood-prone areas prior to a storm's landfall could reduce the number of lives lost and property damage caused by flooding rainfall produced by landfalling TCs. ■

Literature Cited

Aberson, S. D. 1998. Five-day tropical cyclone track forecasts in the North Atlantic basin. *Weather and Forecasting* 13 (4): 1005–15.

AMS. 2000. Policy statement: Hurricane research and forecasting. *Bulletin of the American Meteorological Society* 81 (6): 1341–46.

Ansari, S., and S. Del Greco. 2005. GIS tools for visualization and analysis of NEXRAD radar (WSR-88D) archived data at the National Climatic Data Center. Paper read at the 21st International Conference on Interactive Information Processing Systems (IIPS) for Meteorology, Oceanography, and Hydrology, 12 January 2005, San Diego, CA.

Atallah, E. H., and L. R. Bosart. 2003. The extratropical transition and precipitation distribution of Hurricane Floyd (1999). *Monthly Weather Review* 131 (6): 1063–81.

Barnes, G. M., E. Zipser, D. Jorgensen, and F. D. Marks. 1983. Mesoscale and convective structure of a hurricane rainband. *Journal of the Atmospheric Sciences* 40:2125–37.

Bender, M. A., R. E. Tuleya, and Y. Kurihara. 1985. A numerical study of the effect of a mountain range on a landfalling tropical cyclone. *Monthly Weather Review* 113 (4): 567–82.

Black, M. L., J. F. Gamache, F. D. Marks, C. E. Samsury, and H. E. Willoughby. 2002. Eastern Pacific Hurricanes Jimena of 1991 and Olivia of 1994: The effect of vertical shear on structure and intensity. *Monthly Weather Review* 130 (9): 2291–2312.

Bluestein, H. B., and D. S. Hazen. 1989. Doppler-radar analysis of a tropical cyclone over land: Hurricane Alicia (1983) in Oklahoma. *Monthly Weather Review* 117 (11): 2594–2611.

Cerveny, R. S., and L. E. Newman. 2000. Climatological relationships between tropical cyclones and rainfall. *Monthly Weather Review* 128 (9): 3329–36.

Chan, J. C. L., and X. D. Liang. 2003. Convective asymmetries associated with tropical cyclone landfall. Part I: f-plane simulations. *Journal of the Atmospheric Sciences* 60 (13): 1560–76.

Corbosiero, K. L., and J. Molinari. 2002. The effects of vertical wind shear on the distribution of convection in tropical cyclones. *Monthly Weather Review* 130 (8): 2110–23.

———. 2003. The relationship between storm motion, vertical wind shear, and convective asymmetries in tropical cyclones. *Journal of the Atmospheric Sciences* 60 (2): 366–76.

DeMaria, M., and J. Kaplan. 1994. A statistical hurricane intensity prediction scheme (SHIPS) for the Atlantic basin. *Weather and Forecasting* 9 (2): 209–20.

DeMers, M. N. 2000. *Fundamentals of geographic information systems*, 2nd ed. New York: Wiley.

Dvorak, V. F. 1975. Tropical cyclone intensity analysis and forecasting from satellite imagery. *Monthly Weather Review* 103:420–30.

Elsberry, R. L. 2002. Predicting hurricane landfall precipitation: Optimistic and pessimistic views from the symposium on precipitation extremes. *Bulletin of the American Meteorological Society* 83 (9): 1333–39.

ESRI. 2002. ArcView GIS 3.3. Environmental Systems Research Institute, Redlands, CA.

Franklin, J. L., L. A. Avila, J. L. Beven, M. B. Lawrence, R. J. Pasch, and S. R. Stewart. 2001. Atlantic hurricane season of 2000. *Monthly Weather Review* 129 (12): 3037–56.

Frolov, Y. 1975. Measuring of shape of geographical phenomena: A history of the issue. *Soviet Geography: Review and Translation* 16:676–87.

Gautam, R., G. Cervone, R. P. Singh, and M. Kafatos. 2005. Characteristics of meteorological parameters associated with Hurricane Isabel. *Geophysical Research Letters* 32 (4): Art. no. L04801.

Gilbert, S. C., and N. E. LaSeur. 1957. A study of the rainfall patterns and some related features in a dissipating hurricane. *Journal of Meteorology* 14: 18–27.

Hart, R. E., and J. L. Evans. 2001. A climatology of the extratropical transition of Atlantic tropical cyclones. *Journal of Climate* 14 (4): 546–64.

Hubert, L. E. 1955. Frictional filling of hurricanes. *Bulletin of the American Meteorological Society* 36:440–45.

Jones, R. W. 1987. A simulation of hurricane landfall with a numerical-model featuring latent heating by the resolvable scales. *Monthly Weather Review* 115 (10): 2279–97.

Jones, S. C., P. A. Harr, J. Abraham, L. F. Bosart, P. J. Bowyer, J. L. Evans, D. E. Hanley, B. N. Hanstrum, R. E. Hart, F. Lalaurette, M. R. Sinclair, R. K. Smith, and C. Thorncroft. 2003. The extratropical transition of tropical cyclones: Forecast challenges, current understanding, and future directions. *Weather and Forecasting* 18 (6): 1052–92.

Jorgensen, D. P. 1984. Mesoscale and convective-scale characteristics of mature hurricanes. Part I: General observations by research aircraft. *Journal of the Atmospheric Sciences* 41 (8): 1268–85.

Klazura, G. E., and D. A. Imy. 1993. A description of the initial set of analysis products available from the NEXRAD WSR-88D system. *Bulletin of the American Meteorological Society* 74 (7): 1293–311.

Klein, P. M., P. A. Harr, and R. L. Elsberry. 2000. Extratropical transition of western North Pacific tropical cyclones: An overview and conceptual model of the transformation stage. *Weather and Forecasting* 15 (4): 373–95.

Kruger, A., and W. F. Krajewski. 1997. Efficient storage of weather radar data. *Software-Practice & Experience* 27 (6): 623–35.

Lawrence, M. B., L. A. Avila, J. L. Beven, J. L. Franklin, J. L. Guiney, and R. J. Pasch. 2001. Atlantic hurricane season of 1999. *Monthly Weather Review* 129 (12): 3057–84.

Lin, Y. L., D. B. Ensley, S. Chiao, and C. Y. Huang. 2002. Orographic influences on rainfall and track deflection associated with the passage of a tropical cyclone. *Monthly Weather Review* 130 (12): 2929–50.

MacEachren, A. M. 1985. Compactness of geographic shape: Comparison and evaluation of measures. *Geografiska Annaler* 67B:53–67.

Marchok, T., R. Rogers, and R. Tuleya. 2007. Validation schemes for tropical cyclone quantitative precipitation forecasts: Evaluation of operational models for U.S. landfalling cases. *Weather and Forecasting* 22.

Marks, F. D., G. Kappler, and M. DeMaria. 2002. Development of a tropical cyclone rainfall climatology and persistence (R-CLIPER) model. Paper read at the 25th Conference on Hurricanes and Tropical Meteorology, American Meteorological Society, 29 April–3 May, San Diego, CA.

Matyas, C. J. 2005. Using geographic information systems for the spatial analysis of base reflectivity radar data and applications to the study of tropical cyclone precipitation patterns. Paper read at the 15th Conference on Applied Climatology, American Meteorological Society, 20–23 June, Savannah, GA.

———. 2006. Using annular rings and quadrants to clip polygons representing tropical cyclone precipitation in a geographic information system. Paper read at the 22nd International Conference on Interactive Information Processing Systems for Meteorology, Oceanography, and Hydrology, 29 January–3 February, Atlanta, GA.

———. 2007. Shape measures of rain shields as indicators of changing environmental conditions in a landfalling tropical storm. Working paper, Department of Geography, University of Florida.

Pasch, R. J., L. A. Avila, and J. L. Guiney. 2001. Atlantic hurricane season of 1998. *Monthly Weather Review* 129 (12): 3085–123.

Powell, M. D. 1990. Boundary-layer structure and dynamics in outer hurricane rainbands. 1. Mesoscale rainfall and kinematic structure. *Monthly Weather Review* 118 (4): 891–917.

Rao, G. V., and P. D. Macarthur. 1994. The SSM/I estimated rainfall amounts of tropical cyclones and their potential in predicting the cyclone intensity changes. *Monthly Weather Review* 122 (7): 1568–74.

Rappaport, E. N. 2000. Loss of life in the United States associated with recent Atlantic tropical cyclones. *Bulletin of the American Meteorological Society* 81 (9): 2065–73.

Ritchie, E. A., and R. L. Elsberry. 2001. Simulations of the transformation stage of the extratropical transition of tropical cyclones. *Monthly Weather Review* 129 (6): 1462–80.

Rodgers, E. B., S. W. Chang, and H. F. Pierce. 1994. A satellite observational and numerical study of precipitation characteristics in western North Atlantic tropical cyclones. *Journal of Applied Meteorology* 33 (2): 129–39.

Rogers, R. F., S. S. Chen, J. Tenerelli, and H. E. Willoughby. 2003. A numerical study of the impact of vertical shear on the distribution of rainfall in Hurricane Bonnie (1998). *Monthly Weather Review* 131:1577–99.

Saunders, M. A., R. E. Chandler, C. J. Merchant, and F. P. Roberts. 2000. Atlantic hurricanes and NW Pacific typhoons: ENSO spatial impacts on occurrence and landfall. *Geophysical Research Letters* 27 (8): 1147–50.

Shipley, S. T., I. A. Graffman, and J. K. Ingram. 2000. GIS applications in climate and meteorology. Paper read at the ESRI International User's Conference, 26–30 June, San Diego, CA.

Stoddart, D. R. 1965. The shape of atolls. *Marine Geology* 3:368–83.

Tabachnick, K. E., and L. S. Fidell. 2001. Discriminant function analysis. In *Using multivariate statistics*, ed. R. Pascal, 456–516. Boston: Allyn & Bacon.

Toracinta, E. R., D. J. Cecil, E. J. Zipser, and S. W. Nesbitt. 2002. Radar, passive microwave, and lightning characteristics of precipitating systems in the tropics. *Monthly Weather Review* 130 (4): 802–24.

Tuleya, R. E. 1994. Tropical storm development and decay: Sensitivity to surface boundary-conditions. *Monthly Weather Review* 122 (2): 291–304.

Tuleya, R. E., and Y. Kurihara. 1978. A numerical simulation of the landfall of tropical cyclones. *Journal of the Atmospheric Sciences* 35 (2): 242–57.

Vickery, P. J., P. F. Skerlj, and L. A. Twisdale. 2000. Simulation of hurricane risk in the US using empirical track model. *Journal of Structural Engineering-ASCE* 126 (10): 1222–37.

Vieux, B. E. 2001. *Distributed hydrologic modeling using GIS*. 38 vols. Vol. 38. *Water Science and Technology Library*, ed. V. P. Singh. Boston: Kluwer Academic.

Wentz, E. 2000. A shape definition for geographic applications based on edge, elongation, and perforation. *Geographic Analysis* 32 (2): 95–112.

Wood, E. C. 2001. The analysis and prediction of tropical cyclone rainfall. MS thesis, Department of Meteorology, Pennsylvania State University.

CORENE MATYAS is an Assistant Professor in the Department of Geography at the University of Florida, Gainesville, FL 32611. E-mail: matyas@ufl.edu. Her research interests include severe weather, rainfall patterns, and synoptic climatology.